MedChemComm

RSC Publishing

REVIEW

View Article Online
View Journal | View Issue

Crafting precise multivalent architectures†

Cite this: *Med. Chem. Commun.*, 2013, **4**, 493

Paul M. Levine,[a] Tom P. Carberry,[a] Justin M. Holub[b] and Kent Kirshenbaum*[a]

Received 8th November 2012
Accepted 2nd January 2013

DOI: 10.1039/c2md20338c

www.rsc.org/medchemcomm

Multivalency is a powerful strategy in molecular pharmacology that can establish high-affinity binding between multiple conjoined ligands and corresponding biomolecular targets. Recent advances in chemical synthesis techniques have enabled the development of elaborate two-dimensional multivalent displays appended on natural or synthetic molecular scaffolds. These constructs have the potential to address disease targets that otherwise may be classified as 'undruggable.' In this review, synthetic strategies to generate and functionalize different classes of scaffolds are evaluated. Particular focus is placed on crafting multivalent assemblies that occupy a 'middle space' of molecular weight, along with a consideration of their potential applications in pharmacology.

Introduction

Multivalency can be manifest by multiple conjoined ligands, potentiating their coordinated multi-site association with macromolecular targets (Fig. 1).[1] Relative to monomeric species, multivalent ligand assemblies can collectively exhibit strengthened binding interactions termed 'avidities.' Multivalency plays a critical role in many biological processes, such as viral infection and cell–cell communication.[2,3] The physiological relevance of multivalency has long intrigued biologists and there are currently growing efforts to design chemical tools that can recapitulate these important interactions.

A careful evaluation of the structural requirements necessary to enhance multivalent interactions has been complicated by the arduous synthetic procedures required for precise spatial control of ligand presentation. As a result, multivalent displays have typically exhibited substantial heterogeneity of ligand valency and density. Recent advances in chemical synthesis protocols, however, are now allowing researchers to create complex monodisperse molecular scaffolds with yields and purities that can enable more precise functional characterization. In addition, researchers are now capable of designing molecules that display bioactive ligands, such as carbohydrates and steroid hormones, *via* an array of different two and three-dimensional architectures.[4,5] These advances at the bench have allowed multivalency to emerge as a powerful tool in chemical biology, and facilitate the design of molecules with enhanced binding affinity and specificity for corresponding biomolecular targets. While many multivalent constructs occupy a 'middle space' of medicinal chemistry in terms of molecular weight, they may exhibit desirable attributes compared to small molecules for inhibiting disease targets classified as 'undruggable'.[6] The large surface areas and multiple points of contact often associated with these challenging disease targets, such as protein–protein and protein–nucleic acid interactions, establish an opportunity for developing multivalent assemblies in the discovery of highly specific inhibitors.

In this review, we begin by considering different mechanisms through which multivalent assemblies can bind to their biological targets and provide a brief description of multivalency from a thermodynamic perspective. Our focus is on recent advancements in the design and synthesis of multivalent molecular scaffolds and their various applications in chemical

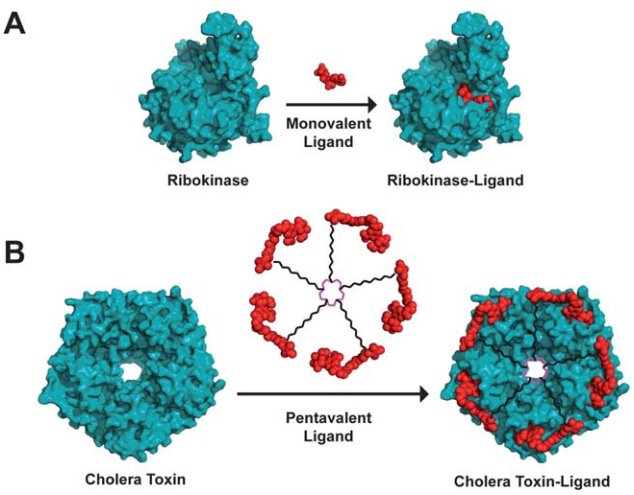

Fig. 1 Structural representations of monovalent and multivalent protein–ligand interactions. (A) Monovalent binding event between *E. coli* ribokinase and the ATP analogue AMP-PCP (PDB ID: 1GQT). (B) Binding event between the B-subunit of cholera toxin and a pentavalent inhibitor (PDB ID: 1LLR). Ligand atoms are shown as red spheres, linker and core atoms are shown as black and magenta lines.

[a]*Department of Chemistry, New York University, New York, New York, 10003, USA. E-mail: kent@nyu.edu*

[b]*Department of Chemistry, Yale University, New Haven, Connecticut, 06520, USA*

† This article is part of the MedChemComm 'Drugs in Middle Space' themed issue.

biology. Due to the large number of reports, this review cannot be comprehensive but specific examples presented are selected as representative in the design of multivalent architectures to target corresponding biomacromolecules. These examples are categorized with regard to different scaffold families. A particular emphasis is placed on multivalent assemblies in 'middle space' (molecules in range of approximately 500 to 3000 Da) and their applications in molecular pharmacology are explored.

Mechanisms of multivalent ligand binding

Multivalent assemblies provide a distinct advantage over monovalent ligands by enhancing binding strength through multiple interactions with their corresponding biological targets.[7] Specific modes of multivalent binding include: statistical rebinding, chelation, clustering, and subsite binding (Fig. 2). In statistical rebinding, the multivalent architecture augments the effective local concentration of ligands near the receptor, producing an overall gain in binding affinity. For example, the tetrameric protein Concanavalin A (ConA), a plant lectin specific for mannose, contains binding sites separated by 72 Å and is an ideal candidate to target with lengthy multivalent assemblies, such as polymers, through statistical rebinding mechanisms (Fig. 2A).[8] Alternatively, the chelate effect is observed when recognition elements bind to multiple receptors, leading to a decrease in the dissociation rate. Chelation can be achieved by bridging adjacent binding sites of target receptors (*i.e.*, AB5 toxins) with multivalent architectures (Fig. 2B). Provided suitable spatial disposition, multivalent assemblies can evoke clustering of multimeric proteins (*i.e.*, cell surface receptors) containing multiple binding sites, significantly enhancing binding affinity (Fig. 2C). Finally, subsite binding occurs between multivalent assemblies and biological targets containing a secondary binding site in proximity to their primary binding pocket, such as nuclear hormone receptors (Fig. 2D). Collectively, these modes of multi-site binding serve to prevent the disassociation of ligand upon individual transient unbinding events.

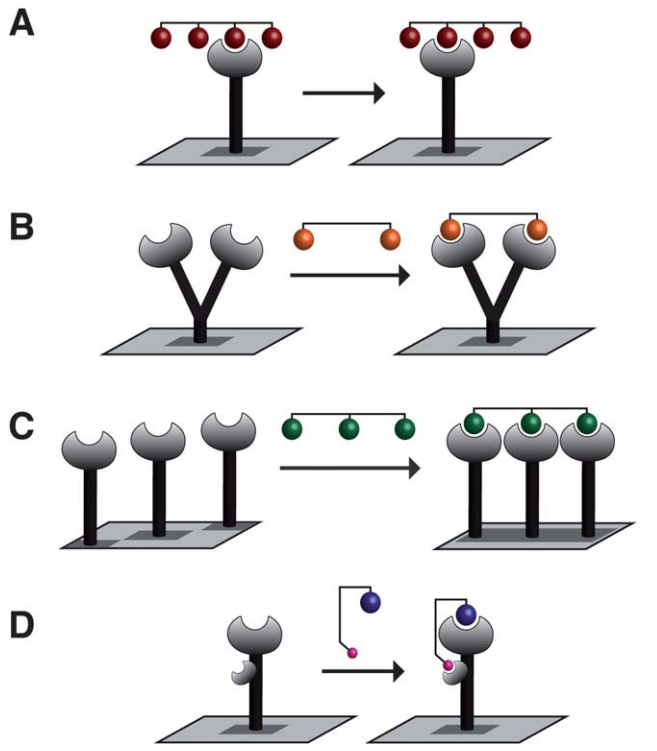

Fig. 2 Specific modes of multivalent binding. (A) Statistical rebinding between a monomeric receptor and a tetravalent scaffolded ligand. High local concentration of ligand enables occupation of the receptor by another ligand upon dissociation. (B) Chelation achieved by bridging adjacent binding sites of a dimeric receptor with a divalent ligand. (C) Clustering of receptors *via* binding of a trivalent scaffolded ligand. (D) Subsite binding between a receptor with a secondary binding site and divalent molecule containing two discrete ligands.

Physical considerations of multivalent effects: a thermodynamic perspective

Numerous research groups have described the physical origins of multivalency from a thermodynamic perspective. Nevertheless, the topologies of the multivalent interactions (spatial arrangement of ligands designed to complement the binding sites of biomolecular targets) and how they contribute to enhancements in binding affinity can remain overlooked.[9,10] Kitov and Bundle have established a thermodynamic model for multivalency incorporating an expression that parameterizes the basis for 'avidity gains' observed in biological systems (Fig. 3A).[11] The first two components of the equation account for enthalpic effects observed in multivalent interactions, and the third component defines a topology-dependent statistical factor termed 'avidity entropy.' More specifically, the first term: $\Delta G^{\circ}_{\text{inter}}$, resembles the free energy of a monovalent interaction ($\Delta G^{\circ}_{\text{mono}}$); the second term: $\Delta G^{\circ}_{\text{intra}}$, constitutes additional specific ligand–receptor interactions; and the third term: $-T\Delta S_{\text{avidity}}$, is a factor that reflects the probability of association

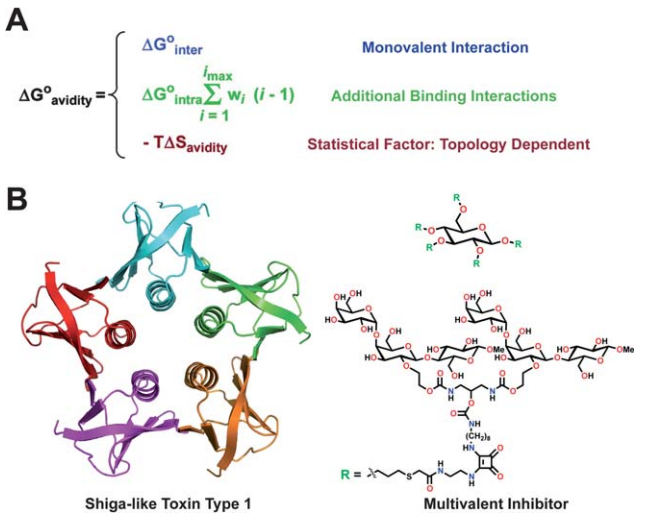

Fig. 3 Physical considerations of multivalent interactions. (A) Thermodynamic model for multivalent interactions between scaffolded ligands and biomolecular targets. (B) Pentavalent carbohydrate inhibitor (right) designed to complement the radial topology of the pentameric subunit of Shiga-like toxin type 1 (SLT-1, PDB ID: 1QNU). Figure adapted from ref. 11.

between each additional ligand and a corresponding binding site. To validate this theoretical model, competitive binding assays were conducted to evaluate the ability of tailored multivalent oligosaccharide assemblies to inhibit the homopentameric binding subunit of Shiga-like toxin type 1 (SLT-1). Relative to the native carbohydrate ligand, which exhibited a 50% inhibitory concentration (IC_{50}) of 0.47 mM, a pentavalent inhibitor designed to complement the radial topology of the pentameric subunit of SLT-1 (Fig. 3B) exhibited an IC_{50} of 1.4 nM. The thermodynamic avidity model calculated an IC_{50} value of 1.26 nM for this ligand–receptor interaction, which was in excellent agreement with the experimentally determined value. These results suggest that the thermodynamics of binding are greatly influenced by the valency and topology of ligand–receptor interactions, and that binding avidities can be quantitatively evaluated using theoretical thermodynamic calculations.[12,13]

Chemical synthesis strategies for generating multivalent architectures

Currently, there are two dominant synthetic strategies to generate multivalent assemblies: sequential and shotgun.[14,15] The sequential approach involves ligating monomeric species in a step-wise fashion to the end of a growing oligomer scaffold (Fig. 4A). This approach is capable of generating highly functionalized multivalent architectures and can yield a monodisperse product. However, the number of synthetic steps is dependent upon the desired number of ligands in the final product, and often requires numerous iterative cycles to generate multivalent displays of preferred density. For this reason, solid phase synthesis techniques are critical to enable construction of multivalent arrays through sequential monomer addition. In contrast to sequential addition, the shotgun method utilizes conjugation reactions to attach multiple identical ligands to pre-existing scaffolds, such as linear polymers or dendrimers (Fig. 4B).[16] Depending on the architecture of the scaffold, the shotgun method can yield highly branched products with ligand valencies exceeding those that are typically attainable through sequential assembly. Due to the high degree of polymerization or incomplete conjugation, however, the shotgun approach often generates polydisperse products, further complicating purification or confounding analysis of biological activity. To create even more elaborate architectures, sequential and shotgun approaches can be combined.[17]

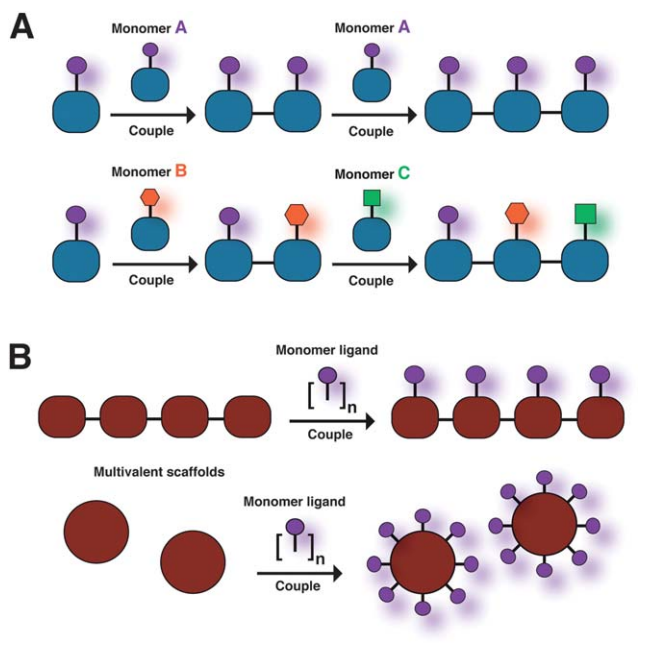

Fig. 4 Synthetic strategies to generate multivalent architectures. (A) Linear multivalent displays can be generated *via* sequential ligation of monomeric units. Products may contain multiple copies of a single ligand (top) or several diverse ligands (bottom). (B) Shotgun approach used to generate linear (top) or radial (bottom) multivalent architectures; monomeric ligands are typically coupled to the scaffold in a single step.

Multivalent platforms

A host of natural and synthetic molecular scaffolds have been designed to address various challenges in biomedicine.[18–24] The size, shape, hydrophobicity and charge of the scaffold are all of crucial importance in determining how these molecules may behave in the context of molecular pharmacology or chemical biology. Important considerations for designing multivalent architectures to target corresponding biomolecules include: ligand valency, density, linker length, three-dimensional spatial arrangement and ability to complement the binding sites of biomacromolecules.[25–27] Depending on the application, other pharmacological characteristics, such as membrane permeability, solubility and proteolytic stability, must also be considered.[28] It is important to note that because the physicochemical characteristics of multimeric interactions vary widely, there is no single ideal scaffold for multivalent ligand displays. In the context of ligand–receptor interactions, careful experimentation must be considered for optimizing multivalent molecular scaffolds in each unique application. Discussed herein are many of the molecular scaffolds families that have been used to craft multivalent architectures; included are evaluations of their applications in molecular pharmacology and chemical biology.

Polymers

Synthetic polymers sample a wide chemical space, from linear macromolecules to highly branched architectures. Polymers are generally polydisperse and can display a wide distribution of molecular weights.[29] The properties of polymeric materials vary widely based on their composition, length, and degree of branching, all of which influence solubility, biocompatibility, rheology, and pharmacokinetic properties *in vivo*.[30] The composition of the polymer scaffold (*e.g.*, linear polysaccharides or polypeptides, poly[norbornenes], *etc.*) influences the structural attributes in solution due to intramolecular hydrogen bonding or ease of solvation, and can alter clearance rates. Although linear synthetic polymer chains generally do not

exhibit well-defined secondary structures, their inherent ability to dynamically span large distances is frequently exploited.

A number of linear polymer conjugates have garnered attention due to their ability to cluster proteins found on the cell surface.[7] Kiessling and co-workers have developed a panel of linear poly(norbornenes) to generate bioactive carbohydrate arrays. Poly(norbornenes) can be synthesized *via* ring-opening metathesis polymerization (ROMP) using Grubbs Ru catalysts.[31–33] This procedure generates polymer products with low polydispersities.[34] The polymers can be synthesized with pendant *N*-hydroxysuccinimide esters, which are readily modified using shotgun-style post-polymerization reactions to afford multivalent, biologically active carbohydrate arrays. Recently, a similar glycomimetic strategy was used to develop multivalent non-carbohydrate inhibitors of DC-SIGN, a membrane-associated lectin capable of recognizing highly glycosylated surfaces of several viral pathogens, including HIV.[35] DC-SIGN was shown to bind weakly to native monosaccharide ligands, such as *N*-acetyl mannosamine and L-fucose, with dissociation constants of 8.7 and 6.7 mM, respectively. Functionalized monovalent shikimic acid conjugates mimicking the core structure of *N*-acetyl mannosamine were screened to identify a ligand with a stronger binding affinity than *N*-acetyl mannosamine. To enhance the binding affinity of the monovalent shikimic acid ligand, the authors used ROMP to generate a multivalent polymer that displayed multiple shikimic acid ligands (Fig. 5). Notably, the multimeric polymer scaffold could engage multiple binding sites of DC-SIGN. The multivalent carbohydrate array enhanced the binding affinity by over 1000-fold ($IC_{50} = 2.9$ μM) relative to monovalent shikimic acid ligands, highlighting the advantage of utilizing multivalent interactions to target cell surface proteins containing multiple binding sites that span large distances and the potential for development of new anti-infective drugs.

Polymers can also be functionalized at the termini to afford dimeric or, in the case of branched polymers, multimeric structures. A report from Kramer and Karpen describes the synthesis of a series of poly(ethylene glycol) (PEG) polymers that are functionalized at each terminus with cyclic guanosine monophosphate (cGMP), a nucleotide capable of binding to multimeric protein receptors located on the cell surface.[36] To investigate the relationship between effects on ligand spacing and binding energy, three variable-length cGMP conjugates were synthesized and evaluated for their ability to bind rat olfactory receptors. The first conjugate, containing a 282-unit PEG chain, was designed with insufficient length required to span the 39 Å distance between the two binding sites. This conjugate displayed only marginally enhanced binding affinity for the receptor target ($K_{½}$ of 0.85 μM *versus* 3.1 μM for the control polymer conjugate containing one cGMP ligand). Incorporating a 3400 unit PEG linker that allowed the divalent construct to bridge the binding pockets of the protein receptor enhanced the binding affinity to 12 nM. In contrast, a 20 000 unit PEG linker significantly longer than the required distance showed a less dramatic increase in binding affinity (250 nM). It has been proposed that long spacers can negatively impact binding affinity of bivalent ligands because the conformation of the products can be compromised due to the collapse of the flexible linker, in addition to influences on chain entropy.[37] These studies highlight the importance of optimizing length when designing scaffolds for bivalent ligand binding.

The chemical versatility that polymer platforms provide for generating multivalent architectures is remarkable. Polymer scaffolds can be tailored to be compatible with a wide range of chemical conjugation strategies. Although polymer conjugates are typically high molecular weight polydisperse products that no longer occupy 'middle space,' their ability to easily span large distances provides a distinct advantage over many other molecular scaffolds for targeting biomolecular assemblies.

Dendrimers

Dendrimers are highly branched macromolecules that generally feature symmetrical spherical architectures.[38] Due to the extent of branching, dendrimers exhibit different properties than linear polymers of similar weight and composition.[30] Unlike

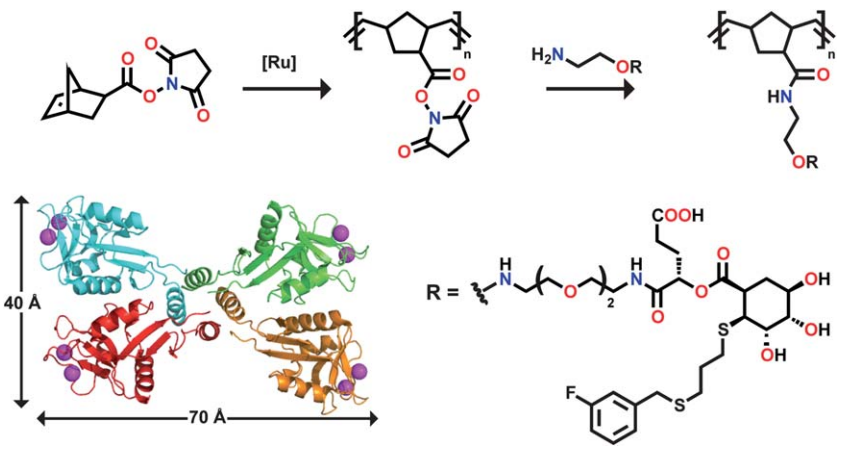

Fig. 5 Synthesis of multivalent non-carbohydrate inhibitors of the membrane-associated lectin DC-SIGN utilizing ring-opening metathesis polymerization (ROMP) techniques. The tetrameric ligand-binding domain of DC-SIGN is shown (ribbon rendered, PDB ID: 1K9I). Calcium ions are represented as purple spheres. Figure adapted from ref. 35.

long-chain linear polymers, dendrimers can be monodisperse and contain a relatively high density of functionalizable termini.[39] The dendrimer termini are typically positioned on the exterior of the globular structure, providing solvent accessibility. The solution-phase structural organization is established primarily by the physicochemical properties of the termini. Dendrimers have been used to enhance the solubility of other molecules, such as ibuprofen.[40] Various functionalizable termini can be included to provide chemical handles to which pendant groups, such as bioactive ligands, can be conjugated.[41]

Multivalent dendritic scaffolds are typically functionalized using a shotgun-style approach. Mass spectrometry or NMR can be used to evaluate the number of conjugated moieties per dendrimer. However, Baker and co-workers have shown that analysing functionalized dendrimers using these methods only provides an average quantifiable weight or structure, which can deviate significantly from the true values.[42] The authors present an example of a G5 poly(amidoamine) dendrimer containing 128 amine termini that were reacted with 14.8 equivalents of ligand to yield an average 12.9 ligands/dendrimer as determined by NMR. By peak-fitting HPLC traces of the compound, however, the authors discovered that the actual functionalized population of the dendrimers followed an approximate Poisson distribution, with only about 10% of the population functionalized with 13 ligands. Strikingly, the authors found that there were members of the dendrimer population that contained as many as 26 ligands or as few as 0.

Dendrimers functionalized with short chain polypeptide sequences have demonstrated potent antiviral activity. Dendrimers are thought to be effective as antiviral agents because they can participate in multivalent binding interactions with corresponding host cells to inhibit viral attachment. A polylysine-based antiviral dendrimer, dubbed SPL7013, is currently undergoing phase III clinical trials as a topical vaginal virucide against HIV-1 under the trade name VivaGel® (Starpharma).[43–46] In addition, Gribaudo and co-workers have shown that a poly(lysine) dendron functionalized with short peptide sequences has antiviral effects against the *Herpesviridae* family.[47] The peptide sequences are enriched in cationic amino acids such as lysine and arginine. The authors hypothesize that the resulting dendrons were able to interact with negatively charged cell membranes and block viral attachment. To test the efficacy of these molecules, Vero cells were pre-incubated with peptide-derivatized dendrons before infection with Herpes Simplex Virus (HSV) type 1 or 2. The IC_{50} of the dendron functionalized with the sequence ASLRVRIKKQ was 0.4 μM against HSV-1 and 1 μM against HSV-2 with respect to viral replication. Interestingly, it was found that pre-treating the cells with a peptide containing a linear lysine core was ineffective against viral replication, suggesting that the multivalent structure of the dendron was necessary for potent antiviral activity.

Dendrimers have also proven effective for preventing bacterial infections. Significant advances in combating infectious bacterial diseases with dendrimeric molecules were recently reviewed.[48] These antimicrobial activities likely rely on multivalent interactions between the dendrimers and the bacterial adhesion factors. In particular, Thompson and Schengrund designed multivalent glycodendritic inhibitors to prevent binding of toxins, such as cholera toxin (*V. cholera*) and heat-labile enterotoxin (*E. coli*) to bacterial cell walls.[49] Binding of these toxins to monosialotetrahexosylganglioside (GM1), a ganglioside present on the host cell surface, induces an array of medical conditions including diarrhea and dehydration.[50] To develop effective inhibitors, polypropylenimine (PPI) and polyamidoamine (PAMAM) dendrimers were synthesized, and functionalized with oligo-GM1 carbohydrate moieties to facilitate interactions with bacterial cell walls (Fig. 6). Radiometric competitive binding assays utilizing ^{125}I-labeled toxins were performed to assess the ability of the multivalent glycodendrimers to inhibit binding of bacteria to the host cell. Relative to the monovalent GM1 ganglioside, the multivalent dendrimers were capable of inhibiting bacterial binding at 1000-fold lower concentrations, establishing the utility of multivalent interactions for preventing bacterial infection. To evaluate the potential therapeutic significance of this class of compounds, the multivalent dendrimers were pre-administered to cell-culture

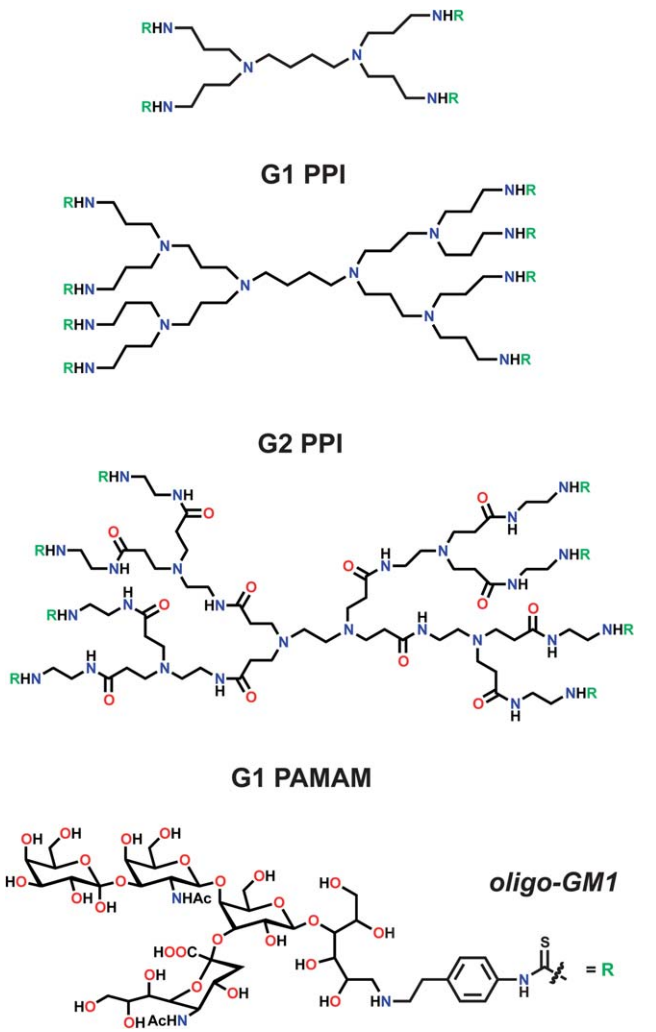

Fig. 6 Polypropylenimine (PPI) and polyamidoamine (PAMAM) multivalent antimicrobial glycodendrimers functionalized with monosialotetrahexosylganglioside (GM1). Figure adapted from ref. 49.

model systems that were subsequently infected with bacterial toxins.[49] Results obtained from these experiments revealed notable reductions in the adherence of ^{125}I-labeled toxins in cells pre-treated with dendrimer. In addition, cell viability was not compromised in the presence of the dendritic compounds, providing evidence that the glycodendrimers could provide a valuable platform for molecular pharmacology.

Dendrimers have enormous utility as platforms for multivalent displays. The work outlined above demonstrates that multivalent dendrimer architectures can be used for a host of purposes, even showing potent antimicrobial and antiviral activities. In addition, multivalent dendritic displays are capable of mimicking natural biological architectures such as liposomes and micelles (*vide infra*). The inherent complications of working with dendrimers (scaffold synthesis and non-specific conjugation), have made it difficult to synthesize and characterize multivalent compounds. Notably, these issues have facilitated the development of analytical procedures (*e.g.*, HPLC) that are now used in the characterization of dendrimers and other multivalent systems.

Nanoparticles

'Nanoparticle' is a broad term that categorizes a range of objects with sizes around the 1 to 100 nm length scale. Many individual macromolecules, such as polymers or spherical metal aggregates, can also be classified as nanoparticles.[51] Gold nanoparticles can easily be synthesized with low polydispersities in a range of sizes, and have shown to exhibit good biocompatibility.[52] Furthermore, gold particles can be readily functionalized in high density by ligands containing thiol groups. It is important to note, however, that metallic nanoparticles used for biological studies should remain chemically inert to avoid toxicity issues *in vivo*. Outfitting metal nanoparticles with multivalent displays can be difficult because they can only be functionalized after they have been pre-formed and their isotropic nature makes site-selective functionalization difficult to control. By contrast, polymeric nanoparticles (*e.g.*, dendrimers or cross-linked polymer micelles) can be designed to display specific functionalities at the periphery or exhibit different morphologies.[53] Although metal and polymer nanoparticles display distinct chemical properties, each has been shown to be applicable in biomedicine and can be used, for example, to develop targeted therapeutics or Magnetic Resonance Imaging (MRI) contrast agents.

Horne, Chen and co-workers utilized the inherent properties of a gold nanoparticle to absorb ionizing radiation for cancer therapy.[54] They report the synthesis of a small molecule-dipeptide hybrid inhibitor of the interaction between poly-SUMO (small ubiquitin-like modifier) and a SUMO-interacting motif (SIM). Molecular recognition between poly-SUMO and SIM has been shown to play a fundamental role similar to ubiquitin in cellular responses to DNA damage, including those caused by cancer radiation therapy.[55] Therefore, augmenting radiation effects or inhibiting DNA damage response may offer a viable therapeutic strategy to sensitize cancer cells without compromising normal cell viability. Virtual ligand screening was used to identify a small molecule-dipeptide hybrid inhibitor of the poly-SUMO and SIM peptide interaction (Fig. 7). The thiol-functionalized inhibitor was conjugated to inert gold nanoparticles (2.0–2.5 nm in size) at up to 100 copies/nanoparticle. While the dipeptide inhibitor was found to be a relatively weak binder on its own (K_d = 1.2 mM), the multivalent gold nanoparticle proved to be very effective at inhibiting the interaction between poly-SUMO and SIM (IC_{50} < 1 μM). To evaluate effects on cell proliferation and radiation response, multivalent gold nanoparticles or control gold nanoparticles, lacking the peptide ligands, were administered to a malignant cancer cell line (MCF-7) or a normal mammary epithelial cell line (MCF-10A). In long-term clonogenic assays, the multivalent gold nanoparticles inhibited growth of MCF-7 cells and enhanced sensitivity to radiation. In addition, the multivalent gold nanoparticles sensitized MCF-7 cells to stress generated by the cytotoxic agent doxorubicin. As expected, the control gold nanoparticles had no impact on either cell line in similar assays. To further validate the observed inhibitory effects, an assay was employed to measure the amount of DNA damage in cells. In comparison to the control gold nanoparticle or untreated cells, a significant

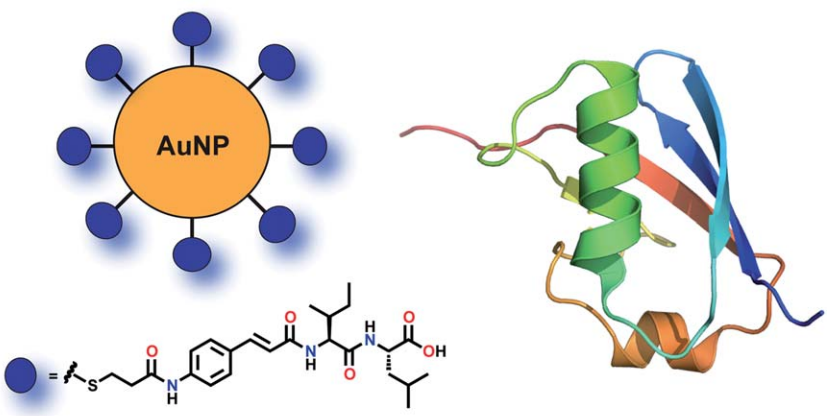

Fig. 7 Multivalent gold nanoparticle (AuNP) inhibitor designed to perturb the binding interaction between SUMO (ribbon rendered, PDB ID: 1QNU) and SUMO-interacting motifs (SIMs). Figure adapted from ref. 54.

increase in damaged DNA was detected for the multivalent gold nanoparticle, suggesting that the repair of damaged DNA is delayed.

Nanoparticles (either metallic or polymeric) can display vastly different chemical properties and have been shown to exhibit good biocompatibility. In particular, gold nanoparticles can be synthesized in a range of sizes with low polydispersities and functionalized in high density by ligands containing thiol groups. Additionally, the inert property of gold provides access to non-toxic materials that are capable of translocating into cells for potential *in vivo* applications. Although nanoparticles are finding frequent use in chemical biology, isotropic particles lead to random display of ligands at low concentrations, potentially compromising binding efficiency.

Carbon nanotubes

Carbon nanotubes are cylindrical graphene materials with high aspect ratios that have recently received considerable attention from the chemical engineering and biomedical communities. Carbon nanotubes are known for their extraordinary strength; nanotubes of around 15 nm in diameter display a tensile strength of approximately 100 GPa.[56] Carbon nanotubes have traditionally found use in the field of molecular electronics, but recently developed chemical functionalization strategies have extended their applications to biomedicine.[57,58] These techniques have allowed the formation of robust tubular scaffolds that present bioactive moieties in an array of patterns suitable for molecular recognition or drug delivery. Simple oxidation of carbon nanotubes in acid is sufficient to establish free carboxylates along the surface of the tube, providing reactive handles for attachment of pendant groups. However, this method has been shown to disrupt the π-network of the conjugated system and adversely impacts the structural integrity of the carbon nanotube.[57,59,60] In contrast, noncovalent supramolecular functionalization of carbon nanotubes can be achieved by exploiting hydrophobic or π-stacking interactions. These strategies are advantageous because the nanotubes can be functionalized in a multivalent fashion without disrupting the π-system and have been used to solubilize carbon nanotubes in both aqueous and organic solvents.[61,62] In addition, recent evidence suggests that hydrophobic interactions between the domains of certain proteins (*e.g.* streptavidin and HupR) and carbon nanotubes can be used to facilitate crystallization of the proteins along the carbon nanotube matrix.[63]

Pyrene has been shown to complex irreversibly to carbon nanotubes through non-covalent interactions. Not surprisingly, these interactions have been exploited to functionalize carbon nanotubes with a multitude of pyrene derivatives.[64] Khiar and co-workers recently reported a modular approach to outfit carbon nanotubes with carbohydrate ligands in a multivalent fashion for the development of nanomaterials that can engage in specific ligand–lectin interactions.[65] These multivalent assemblies show potential for targeting cell surface lectins that play a critical role in numerous biological processes, including tumour cell metastasis and pathogen infections.[66] The authors developed an efficient protocol to readily synthesize an array of carbon nanotubes functionalized with glycoconjugates containing distinct functionalities. Sugar moieties were conjugated to variable azido-functionalized hydrophilic PEG spacers *via* amide bond formation. Subsequent CuAAC chemistry between the azide linker and pyrene containing a terminal propargyl moiety allowed for attachment of these conjugates to carbon nanotubes *via* non-covalent interactions (Fig. 8). Carbon nanotube assemblies synthesized using similar methods, but containing lactose epitopes, were investigated to determine if they would provide a molecular platform for specific ligand–lectin recognition. Lactose epitope-functionalized nanotubes

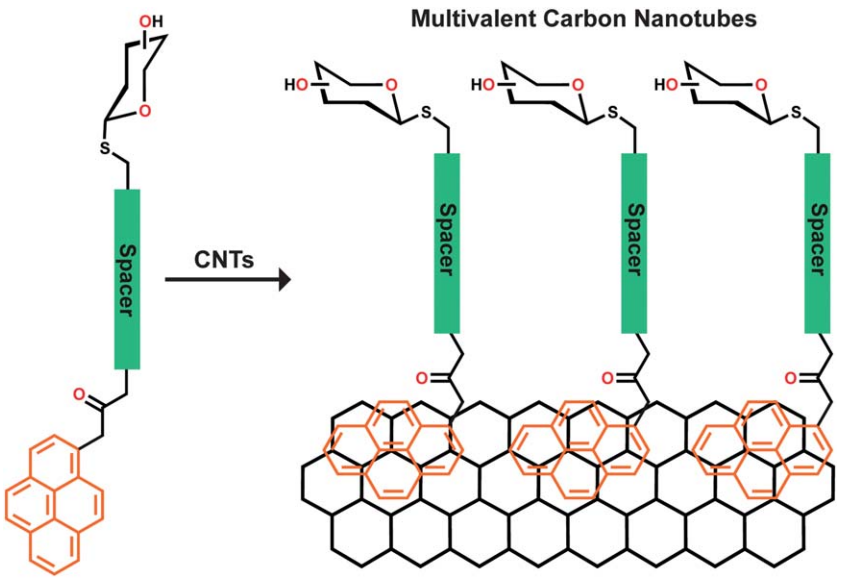

Fig. 8 Non-covalent synthetic strategy used to generate carbon nanotubes functionalized with distinct carbohydrate moieties (CNT: carbon nanotube, schematically depicted at bottom right). Figure adapted from ref. 65.

were incubated with a fluorescein-labeled plant lectin specific for lactose and fluorescence spectroscopy was conducted to determine specific binding. The lactose-containing multivalent conjugates were capable of recognizing *Arachis hypogaea* peanut agglutinin, as indicated by a fluorescence signal. To verify specificity, the authors performed a control experiment with a multivalent carbon nanotube displaying mannose epitopes. As expected, no fluorescence tagging was detected for the mannose conjugate, confirming that the receptor is specific for lactose epitopes.

Carbon nanotubes have become ubiquitous in many disciplines of research. Unlike planar or even spherical multivalent arrays, nanotubes provide an elongated cylindrical molecular recognition platform that can be variably rasterized in two separate dimensions (curvature and length) and may ultimately assist in optimizing certain multivalent interactions. Additionally, carbon nanotubes can be functionalized utilizing both covalent and non-covalent strategies, although disruption of the π-network can induce structural degradation and compromise biological integrity.

Virus capsids

Viral capsids, or protein coats, are comprised of multiple protein subunits that generally form three-dimensional helical or icosahedral structures. Virus-like particles are typically monodisperse and biodegradable, effectuating their use in biomedical applications.[67] Furthermore, the external or internal surface of the viral protein coat can be functionalized to display multiple copies of distinct targeting molecules or therapeutic agents. Viral capsids are often synthesized *via* recombinant expression in *E. coli*, creating self-assembling products.

Finn and co-workers have generated variants of the *Levivirus* bacteriophage Qβ capsid that are capable of acting as therapeutic delivery vehicles.[68] The capsids (28 nm in diameter) were functionalized with multiple copies of the epidermal growth factor (EGF) protein to effect binding to the EGF receptor on the surface of cells. Formation of the modified capsids was accomplished by co-expressing a truncated version of the native coat protein with a second protein containing a C-terminal EGF domain in *E. coli*. These capsids displayed an average of 5–12 EGF domains on their surface. To add additional imaging tags, the capsid surface was subsequently functionalized with fluorescent tracers *via* lysine residue amines. *In vitro* tests with A431 (epidermoid carcinoma) cells, which overexpress the EGF receptor, revealed that the modified capsid structures were able to bind with high affinity, as quantified by confocal fluorescence microscopy. Importantly, wild-type capsids lacking EGF domain ligands bound weakly and produced little to no activity. The modified capsids were also able to induce EGFR phosphorylation cascades and eventually apoptosis, although these results were only observed at high concentrations.

Synthetically modified viral capsids have also been used as MRI contrast agents.[69–71] Gadolinium chelates were conjugated to the interior or exterior of MS2 viral capsids, generating structures that displayed approximately 90 ligands per capsid. Interestingly, the virus-like particles with contrast agents on the interior surface exhibited a higher relaxivity than their externally functionalized counterparts (41.6 mM^{-1} s^{-1} *vs.* 30.7; 30 MHz, 298 K). The authors concluded that water is able to diffuse into the capsid and that the rigidity of the capsid interior enhanced the observed relaxivity.[71]

Nature has endowed viral capsids with the ability to display ligands in a multivalent fashion. Viral capsids are advantageous scaffolds compared to other multivalent platforms because of their intrinsic biocompatibility. The ability to functionalize viral capsids represents a unique opportunity for chemists to expand their synthesis techniques to include biomacromolecular assemblies as substrates. The display of multiple ligands in well-defined topologies should facilitate the development of designed multivalent architectures on the same large length scales as viral capsids themselves.

Supramolecular scaffolds

The field of supramolecular chemistry is based on strong, directional, non-covalent interactions that are exploited to build complex, multi-component assemblies. Importantly, the interactions that hold supramolecular scaffolds together are often reversible, allowing multivalent architectures of this nature to be assembled or disassociated using subtle changes in environment.[72,73] Supramolecular interactions include hydrogen bond donor-acceptor systems (*e.g.*, nucleobase recognition in DNA), metal coordination motifs (*e.g.*, histidines coordinating to iron in porphyrin ring systems), and hydrophobic host–guest interactions (*e.g.*, substrates being associated with enzyme binding pockets). The reversible nature of supramolecular complexes can facilitate functionalization strategies. In addition, supramolecular chemistry provides access to scaffolds capable of adopting a myriad of topologies, thus establishing the potential to interact with multiple biomolecular targets.

Seeberger has introduced modular small molecule scaffolds that are capable of displaying carbohydrates with a 'tunable' spatial arrangement.[74] These starburst-like molecules (dubbed RuCDMan) rely upon metal coordination and host–guest interactions to form self-assembled supramolecular multivalent complexes. The compounds are generated from a fluorescent ruthenium(II) (2,2-bipyridyl) core conjugated to six adamantyl units that can recognize mannosylated β-cyclodextrin, forming a supramolecular complex (Fig. 9). These RuCDMan complexes were evaluated for their ability to bind ConA using surface plasmon resonance (SPR). Increasing the valency of the recognition elements from 14 to 28 mannose units enhanced binding affinity (K_d) approximately 2-fold, from 0.23 μM to 0.14 μM respectively. Notably, the complex displaying six adamantyl units (42 mannose units) did not exhibit an increase in binding affinity, presumably due to the steric congestion of the complex on the surface, but was found to bind to bacterial pili. The binding specificity of the supramolecular assembly was evaluated using two strains of *E. coli*, one expressing mannose-specific adhesion proteins in their pili, and the other without. As expected, the complex only bound to bacteria displaying the mannose-specific pili. Binding of the supramolecular complex was quantified using the inherent fluorescence of the

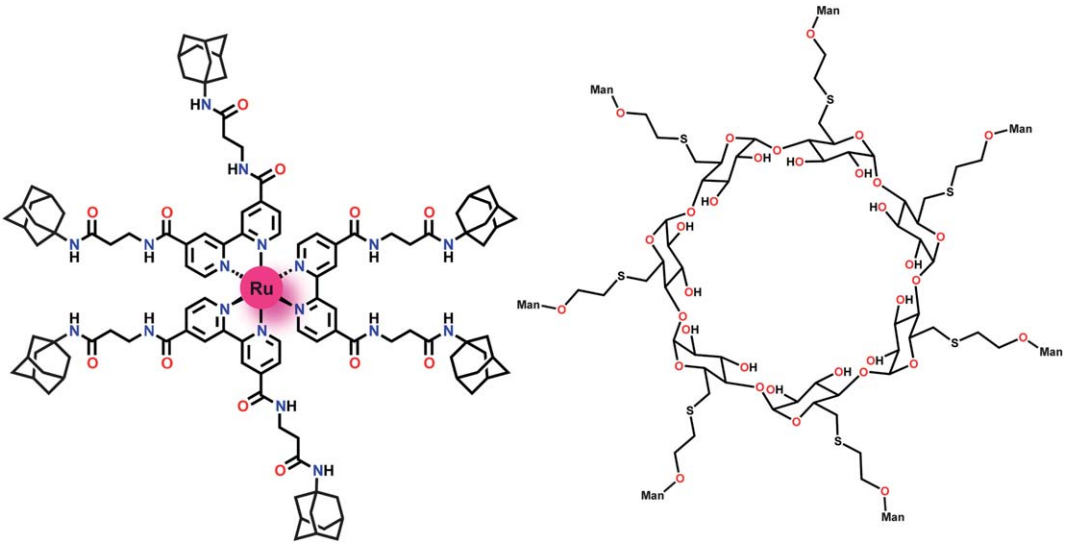

Fig. 9 Self-assembled supramolecular multivalent complexes containing adamantyl units (left) capable of recognizing mannosylated β-cyclodextrin (right). Figure adapted from ref. 74.

ruthenium core. Furthermore, the non-covalent nature of the β-cyclodextrin host–guest complex allows for the targeting moiety to be exchanged, making this specific supramolecular complex useful for a wide range of multivalent binding and sensing applications.

Supramolecular polymers are polymeric structures constructed from non-covalently linked units, and have been shown to reversibly associate with specific targets. Müller and Brunsveld have reported the synthesis of a disc-shaped macromonomer that displays up to three mannose units at the peripheral surface.[75] The discs are comprised of an aromatic core containing PEG side chains that can reversibly assemble into fibril columns at low concentrations in aqueous conditions. As the monomers associate, the polymer becomes increasingly fluorescent. The mannosylated polymers were shown to bind ORN178 bacteria, an *E. coli* strain that displays a mannose-specific adhesion (*FimH*), as indicated by a strong fluorescent response. Tests in dilute bacterial suspensions revealed the bacteria could still participate in bacterial clustering, supporting the view that the supramolecular polymers were able to function as long polyvalent scaffolds in order to engage in multivalent interactions with several bacteria and cause aggregation. Unlike linear polymers, however, the dynamic supramolecular complexes were shown to spontaneously de- and re-polymerize, forming assemblies with ligand densities corresponding to the substrate. Interestingly, copolymerization of the mannosylated discs with unfunctionalized discs showed that lower ligand densities were more effective at bacterial recognition. Furthermore, it was found that addition of a 10^6-fold excess of mannose did not abrogate binding of the polymer to the bacteria, indicating that the multivalent supramolecular architectures produced strong interactions. A recent report from the Scherman group expanded upon this concept by using a flexible covalent backbone to allow the polymer to adopt to the native binding surface.[76] The side chains were functionalized with naphthyl units that could complex with glycosylated cucurbituril and allow for a similar selection based on active site spacing.

Supramolecular scaffolds are distinct among other multivalent architectures discussed in this review due to their extremely versatile assemblies and intrinsic reversibility. The ability to fine-tune the scaffold during synthesis allows for a host of ligands to be displayed on the surface that can even be exchanged for other ligands *in situ*. These synthetically facile and robust molecular scaffolds can also adopt different three-dimensional architectures, establishing the potential to engage in distinct binding interactions with biomolecular targets.

Multivalent lipid complexes

Liposomes and micelles are semi-synthetic nanoparticles composed of amphiphilic phospholipid aggregates. Lipid complexes are considered as potential therapeutics due to their biodegradability and non-immunogenicity. However, they are susceptible to rapid clearance from circulation.[77] Liposomes resemble structures of compartmented biological membranes at their most fundamental level. The solvent exposed hydrophilic surfaces of liposomes have been used to display a host of recognition elements to facilitate intracellular uptake.[78] In addition, their aqueous cores can sequester various bioactive compounds (*e.g.*, doxorubicin in the product Doxil®). Although the overall size of these particles can be nearly homogeneous in solution, control of the spatial disposition of the recognition elements on the liposome surface can be difficult to control due to the fluid nature of the phospholipid bilayer.[79] In contrast, micelles are spherical phospholipid complexes that lack an internal aqueous cavity. These lipid complexes can be synthesized from purely unnatural components. For example, amphipathic dendritic structures can form unimolecular micelles.[80] Additionally, block copolymers that phase-separate into a hydrophobic inner region and a hydrophilic outer region have been shown to form micellar structures.[81] Similar to

liposomal assemblies, the hydrophilic surfaces of micelles can be tailored to establish biological functions, making these assemblies particularly useful for applications in drug delivery. The ability of liposome and micelle architectures to display multiple ligands should facilitate the development of artificial multivalent architectures that mimic the dimensions and physicochemical properties of biological membrane-delineated compartments.

Polypeptides

Proteins often utilize conformationally defined domains to engage biomolecular targets.[82] Unfortunately, synthetic oligomers are often restricted in their ability to fold into discrete secondary and tertiary structures. Short oligopeptides offer a route to obtain biologically active compounds that are easily synthesized and are capable of forming stable secondary structures that will recognize biological targets.[83,84] Indeed, the ability to control the topology of the peptide backbone has enabled researchers to engineer peptides that target a wide range of proteins and nucleic acids.[85]

The interactions between CD40, a constitutively active protein expressed on the surface of dendritic cells, and its native glycoprotein ligand CD40L play a fundamental role in cellular immune responses.[86,87] Similar to other transmembrane proteins in the tumor necrosis factor receptor (TNFR) superfamily, CD40 relies upon self-assembly to form three-fold symmetric, non-covalent homotrimers for intracellular signaling.[88] Selective modulation of CD40–CD40L signaling may lead to new therapeutic agents that can combat immunologic diseases or malignancies.[89–91] Using X-ray crystal structures, homology models and 'hot spot' residues of CD40L as guides, the Guichard group has synthesized functional CD40L mimetics from cyclic and branched peptides that adopt native homotrimeric assemblies (Fig. 10).[92] In competitive binding experiments utilizing surface plasmon resonance analysis, a cyclic and a branched peptide exhibited IC_{50} values in the nanomolar and micromolar ranges, respectively. Competitive binding was not observed using negative control sequences, including the linear variants of the C_3-symmetric cyclic peptides. This result highlights the importance of controlling the conformation of the scaffold to enhance binding energy through multivalent interactions (*vide supra*).

More recently, an on-bead high-throughput screening platform was developed to identify peptides that inhibit protein–nucleic acid interactions.[93] It is known that the association between *trans*-activation response (TAR) element RNA and Tat, a protein that enhances transcription of HIV-1, plays a fundamental role in viral replication.[94,95] The Tat–TAR complex is therefore an attractive target for the development of new anti-HIV therapies. Although significant efforts have been devoted to developing inhibitors of the Tat–TAR interaction, most therapeutic agents lack the ability to establish a surface area large enough to inhibit the interaction with sufficient potency and selectivity.[96,97] Seeking to take advantage of multivalent interactions, the Santos group has synthesized branched peptides containing amino acids that are capable of forming multiple non-covalent interactions with RNA. Initial screening efforts to identify peptides that bind to TAR RNA yielded 17 'hits' that were subsequently validated by dot blot assays. The most effective branched peptide sequence exhibited a dissociation constant of 0.6 μM. Truncation of the branched peptide into its linear counterpart significantly decreased binding affinity by >125-fold, suggesting that multivalent interactions are indeed responsible for enhanced affinity. To assess the selectivity of the branched peptide, TAR RNA sequences containing point mutations were synthesized. Modification of the native TAR RNA tertiary structure decreased binding affinity by approximately 10-fold, indicating that the branched peptide is selective for the TAR RNA structure.

Peptides offer a versatile platform from which to develop three-dimensional multivalent architectures. The modularity of the peptide scaffold allows for the generation of finely tuned sequences that can be tailored to a multitude of biomacromolecules. Some attributes of peptides may limit applications in chemical biology and pharmacology, such as

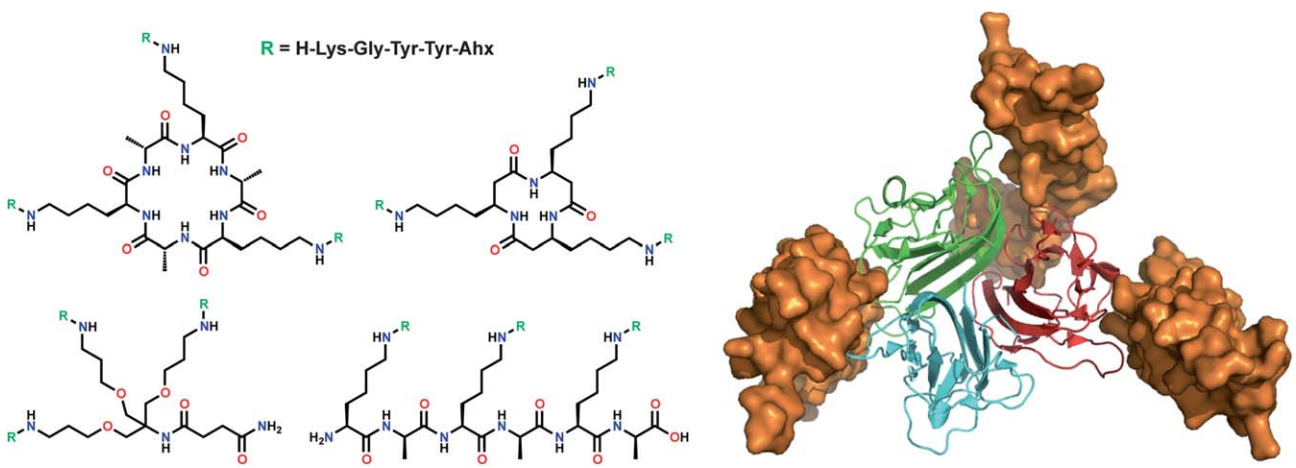

Fig. 10 Trivalent multivalent peptide inhibitors designed to disrupt the binding interaction between trimeric CD40 (ribbon rendered, PDB ID: 3QD6) and CD40L (surface rendered). Figure adapted from ref. 92.

susceptibility to proteolytic degradation and poor cell permeability. However, efforts to identify encodable signals within short peptide sequences that facilitate uptake and delivery to specific cellular compartments are now being pursued.[98] Once these signals are identified, they may be used to enhance the permeability and trafficking of multivalent peptide assemblies within cells.

Peptide nucleic acids

Peptide nucleic acids (PNAs) are uncharged and achiral polyamide oligomers that contain nucleobase side chains. These synthetic oligomers lack the sugar-phosphate backbone of traditional nucleic acids, such as RNA or DNA, and can be designed to complement specific oligonucleotide sequences. In particular, molecular recognition between PNAs and single-stranded DNA or RNA offers an intriguing opportunity to display bioactive ligands in a multivalent fashion because the spatial arrangement of the individual ligands along helical backbone can be controlled with a high degree of precision.[99] Hybridization *via* complementary Watson–Crick base-pairing results in molecular entities containing high affinity and sequence selectivity, providing access to monodisperse products.[100] In addition, the abiotic backbone of PNAs makes this molecular scaffold resistant to proteolytic degradation.[101] Although PNAs posses numerous advantageous chemical properties, their intracellular applications may be limited due to poor membrane permeability.[102]

The Appella group recently introduced a general strategy for synthesis of multivalent architectures that display receptor ligands on novel PNA scaffolds to target $\alpha_v\beta_3$ integrins.[103] The core of the scaffold is a hybrid between a PNA and single-stranded DNA (Fig. 11). The overexpression of $\alpha_v\beta_3$ integrins plays a fundamental role in metastasis of certain cancers as these recognition elements mediate cell attachment through multivalent binding events between peptides located in the extracellular matrix.[104,105] Cells that overexpress $\alpha_v\beta_3$ are often targeted by synthetic small molecules that bind integrin through monovalent binding interactions. These approaches, however, often lack selectivity, compromising potency.[106,107] A library of γ-substituted L-lysine PNAs covalently attached to cyclic RGD-motif containing peptide ligands have been synthesized and were used to block the attachment of metastatic melanoma cells to an extracellular matrix both *in vitro* and *in vivo*. In radiolabeled competitive binding assays, a multivalent DNA:PNA complex containing fifteen cyclic RGD ligands (DNA:PNA-D_5) exhibited a dissociation constant two orders of magnitude lower than the monovalent cyclic RGD ligand (0.16 *vs.* 62.9 nM, respectively). In addition, DNA:PNA-D_5 suppressed tumor colonization in the lungs of mice by approximately 50% relative to control treatments. These results confirm that multivalent DNA:PNA complexes can be designed to enhance binding affinity and biological activity.

Solid phase synthesis techniques enable rapid generation of PNA oligomers that can hybridize to nucleic acids with high affinity and specificity. Moreover, molecular recognition provides a unique and advantageous platform to assemble monodisperse multivalent architectures with control over spatial arrangement of the individual ligands. These artificial polymers are more resistant to proteolytic degradation compared to similar length peptides, although cell permeability still remains a potential impediment.

Peptoids

The directed assembly of multivalent displays on a modular oligomer framework enables control over important physicochemical features of the product molecules.[108] For example, scaffold conformation, size, charge and branching all influence the pharmacological profile of the products. The ability to control these characteristics by the sequence-specific synthesis of biocompatible oligomers imparts a great advantage in the design, generation, and testing of the products for therapeutic or biomaterials applications.

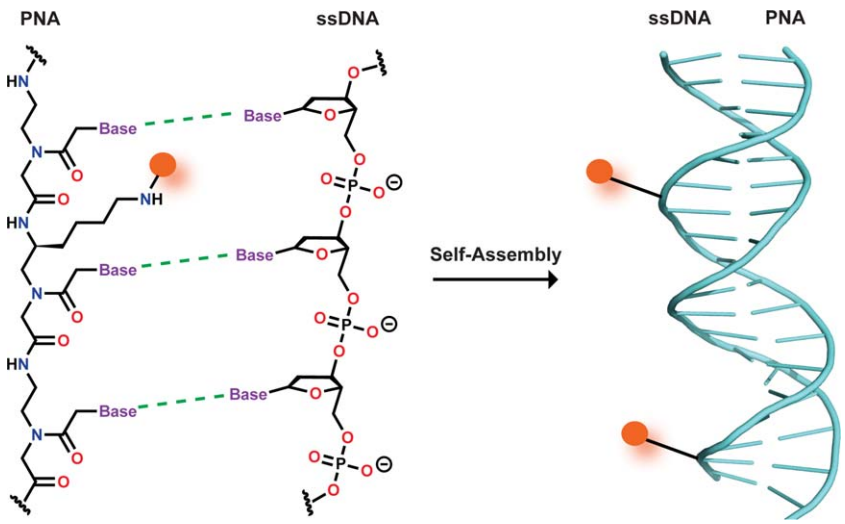

Fig. 11 Chemical structure of a γ-substituted L-lysine peptide nucleic acid motif bearing a $\alpha_v\beta_3$ integrin recognition ligand (depicted as orange circle) bound to DNA. Figure adapted from ref. 103.

N-Substituted glycine oligomers, or 'peptoids,' are a class of peptidomimetics composed of tertiary amide linkages. Peptoids are notable for their facile synthesis, synthetic diversity, and ability to fold into distinct secondary structures.[109–115] Unlike peptides, peptoids readily populate *cis* amide conformers and contain no amide NH groups, engendering proteolytic stability and enhanced cell permeability.[116,117] In addition, sequence-specific assembly of peptoid oligomers on solid support provides access to monodisperse products, a distinct advantage over other molecular scaffolds, such as random polymers.[118]

Recent studies in the Kirshenbaum group have reported novel approaches to functionalize peptoid oligomers. Initially, linear peptoid oligomers were used as substrates for the CuAAC reaction to conjugate chemically diverse pendant groups, including nucleobases and fluorophores, at up to six positions along to the oligomer backbone with high efficiency (Fig. 12A).[119] Following these studies, peptoid oligomers were functionalized with up to four distinct moieties through sequential steps of conjugation and oligomer extension (Fig. 12B).[120] The use of sequential conjugation strategies enabled the development of heterogeneous displays. This conjugation strategy has provided a foundation to generate multivalent peptoid displays capable of targeting diverse biomacromolecules.

To investigate potential biomedical applications of peptoid assemblies, steroid ligands that modulate the activity of nuclear hormone receptors were conjugated to peptoid substrates.[121] Nuclear hormone receptors, such as the estrogen receptor (ER), bind to their native steroid hormones, dimerize, translocate into the nucleus, and bind specific DNA sequences to regulate gene expression.[122–125] Overexpression of the ER has been linked breast and ovarian cancers, making it an important therapeutic target. Peptoid bioconjugates functionalized with ER ligands, termed estradiol peptidomimetic conjugates (EPCs), were synthesized and evaluated for their ability to competitively bind the ER. In radiometric competitive binding assays using whole cell lysates, EPCs containing one or six steroid ligands exhibited 50% effective concentration values of 2.47 μM and 10.9 nM, respectively.[126] Increasing the valency of the estradiol pendant groups significantly enhanced binding affinities of the EPCs, consistent with multivalent interactions. Studies were also conducted on EPCs to evaluate effects of valency and spacing on ER-mediated transcriptional activation.[127] Notably, these studies highlight the ability for multivalent ligands to modulate intracellular receptor activity in a length- and valence-dependent manner.

More recently, conformational constraints were introduced into peptoid oligomers to expand the utility of this scaffold as a multivalent chemical platform (Fig. 13).[128] Bioactive androgen receptor (AR) ligands, such as ethisterone, were conjugated to cyclic and linear peptoid scaffolds and the effects of valency, spacing and conformational ordering on AR activity were evaluated. The AR is an important drug target and there is a critical unmet need to develop new therapeutic regimens for treatment of castrate-resistant prostate cancer.[129] It was demonstrated that increasing the valency and spacing of the ethisterone ligands enhanced binding and AR-mediated transcriptional activation in a length- and valence-dependent manner, consistent with

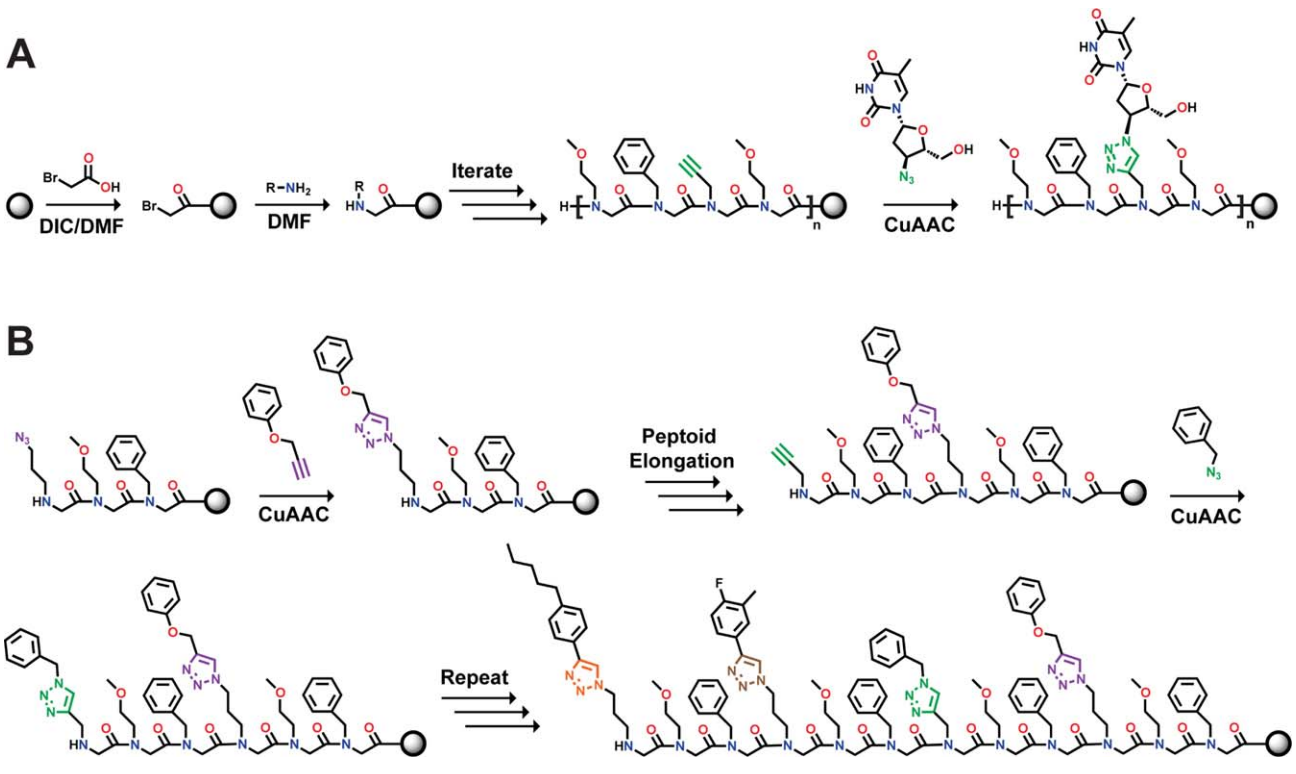

Fig. 12 Synthesis of (A) mono-functionalized and (B) poly-functionalized multivalent peptoid oligomer conjugates though copper-catalyzed azide–alkyne [3 + 2] cycloaddition reactions conducted on solid support. Figure adapted from ref. 119 and 120.

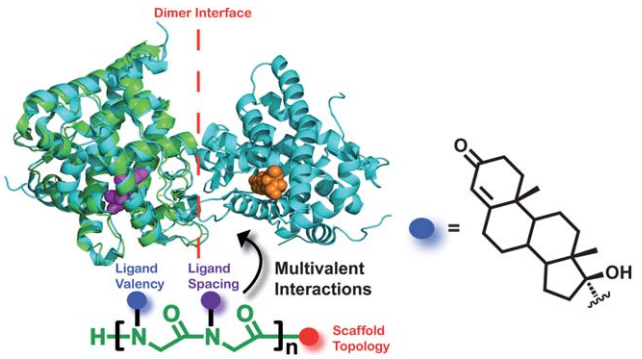

Fig. 13 Multivalent peptoid oligomers bearing reactive ethisterone ligands capable of modulating androgen receptor activity through multivalent interactions. Colored circles represent sites amenable to chemical modification and ligand display. Homology model of the AR ligand binding domain dimer (PDB: 1I37) bound to native ligand (DHT-*magenta*). Figure adapted from ref. 128.

previously reported multivalent interactions. In cell-based proliferation assays modeling castrate-resistant prostate cancer, both a linear and a cyclic conjugate were shown to possess potent anti-proliferative activity through distinct mechanisms of action.[130] These results highlight the versatility of the multivalent chemical platform to modulate AR activity and potential to circumvent drug resistance in AR pharmacology.

Additional work on peptidomimetic oligomers for multivalent display by the Disney lab includes the development of modularly assembled peptoid oligomers to target RNA internal loop motifs implicated in myotonic dystrophy type 1 (DM1) and type 2 (DM2).[131] DM1 and DM2 result from the expansion of triplet CTG and quartet CCTG repeats in the *DMPK* and *ZNF9* genes, respectively, making these repeating motifs pharmaceutically relevant targets for multivalent assemblies.[132–135] It has been shown previously that similar RNA internal loop sequences bind bis-benzimidazole (or Hoechst 33258).[136] To this end, peptoid oligomers were used as a molecular scaffold to display up to five terminal alkyne moieties and conjugated to azido-functionalized bis-benzimidazole RNA recognition elements using the CuAAC reaction (Fig. 14A). Notably, increasing the valency from two to five RNA recognition elements and proper spacing of the conjugates enhanced binding affinity and specificity for RNA sequences associated with DM1.[137] The dimeric and pentameric conjugates exhibited binding affinities of 100 and 13 nM, respectively. In addition, recent evidence indicates that conjugates containing bis-benzimidazole RNA recognition elements are potently bioactive at concentrations as low as 2.5 μM in cell culture model systems.[138] The potent bioactivity demonstrates the therapeutic potential of modularly assembled peptoid oligomers for applications in molecular pharmacology.

Using similar design strategies, peptoid-based aminoglycoconjugates were synthesized utilizing 6′-*N*-5-hexynoate kanamycin A ligands, an aminoglycoside antibiotic, to target RNAs that cause DM2 (Fig. 14B). Aminoglycoconjugates

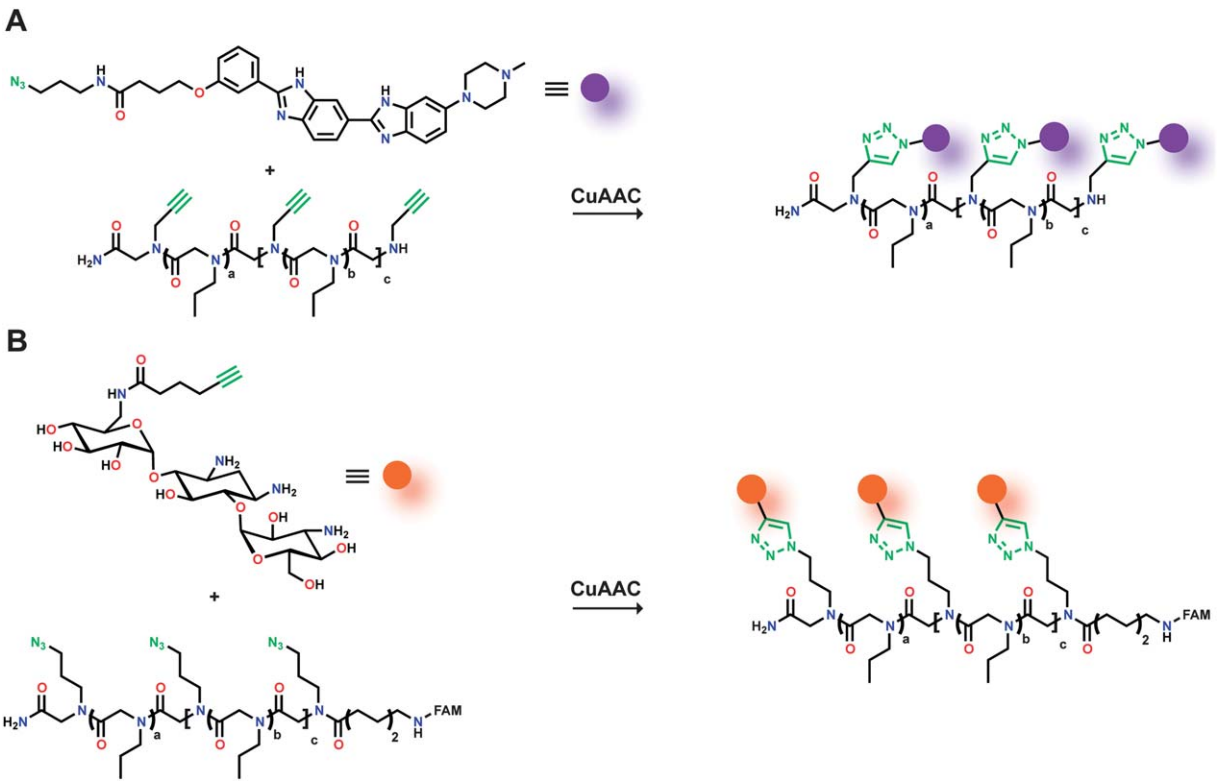

Fig. 14 Modularly assembled peptoid oligomers that target RNA internal loop motifs implicated in myotonic dystrophy type 1 (DM1) and type 2 (DM2). (A) Anchoring of bis-benzimidazole RNA recognition elements using the copper-catalyzed azide–alkyne [3 + 2] cycloaddition reaction to target RNA involved in DM1. (B) Anchoring of 6′-*N*-5-hexynoate kanamycin A RNA recognition elements using the copper-catalyzed azide–alkyne [3 + 2] cycloaddition reaction to target RNA involved in DM2. FAM indicates position of coupled 4(5)-carboxyfluorescein. Figure adapted from ref. 137 and 140.

containing up to three 6′-*N*-5-hexynoate kanamycin A RNA recognition elements were shown to bind with high specificity to their intended RNA target.[139] Increasing the valency from two to three 6′-*N*-5-hexynoate kanamycin A moieties exhibited binding affinities of 50 and 8 nM, respectively. In addition, the ability to control the spacing between the RNA recognition elements can convert aminoglycoconjugates selective for DM2 RNA into those selective for DM1 RNA, a result that is uniquely attributed to sequence control for these oligomeric molecular scaffolds.[140]

The modular assembly of peptoid oligomers allows for the installation of many orthogonal side chain functional groups, a distinct quality that can be utilized to conjugate an array of bioactive ligands and to optimize biological activity. This characteristic, and the ability to alter the topology of the peptoid scaffold, creates a versatile molecular platform to generate a wide variety of three-dimensional multivalent architectures. Overall, solid phase synthesis techniques permit the sequence-specific assembly of peptoid oligomers, providing access to monodisperse products with control over valency and spacing.

Conclusion

There is a growing appreciation for exploration of a 'middle space' in molecular pharmacology (*i.e.*, bioactive compounds with molecular weights between 500 and 3000 Daltons). As reviewed above, multivalent displays are beginning to play a critical role in these discovery efforts. Classically, small molecules with molecular weights below 500 Daltons have been considered as the most suitable for clinical implementation.[137] X-ray crystallography has played a prominent role in these efforts by elucidating small molecule drug–target interactions. Nevertheless, it is now apparent that certain biomolecular targets may be 'undruggable' by small molecules, either because of the difficulty of identifying individual ligands with sufficient binding strength, or because of the large surface areas required to antagonize targeted interactions.

Over the past several decades, multivalent displays presenting bioactive ligands have emerged as a potential family of therapeutics. Initial efforts focused on the development of random polymers and other polydisperse high molecular weight constructs to engage in high-affinity binding events with biomolecular targets.[1] These multivalent assemblies successfully enhanced binding strength through avidity effects and still hold promise as effective antagonists of macromolecular interactions that are manifest over large surface areas.

Intriguing sets of new studies have begun to explore the possibility of crafting more precise multivalent displays. Advances in chemical synthesis techniques, such as solid phase protocols and orthogonal conjugation strategies, have enabled chemists to functionalize a plethora of molecular scaffolds, providing access to monodisperse products with control over ligand valency and spacing. These elaborate three-dimensional multivalent architectures are capable of complementing the binding sites of corresponding biomacromolecules.

To date, there have been only limited examples of multivalent therapeutics. Three main advantages of utilizing monodisperse multivalent assemblies include: improved control over the pharmacological properties of the construct (including PK/PD and off-target effects), greater understanding of the structural requirements for optimizing binding interactions, and an opportunity to facilitate clinical trials and regulatory approval. These advantages will play a crucial role in the future development of multivalent therapeutics.

Increasingly, it appears that 'middle space' offers a sweet spot for crafting precise multivalent displays. In the future, we may begin to see additional examples of monodisperse multivalent displays in which high-resolution structural studies enable the types of structure–activity studies that have been the mainstay of small molecule drug discovery efforts. More importantly, these monodisperse multivalent constructs hold great promise to address challenging disease targets that otherwise may be classified as 'undruggable.' Although the first clinical trials using drugs derived from multivalent architectures are now beginning to appear, the small molecule paradigm of the pharmaceutical industry will surely adapt to include new chemical entities that occupy 'middle space' in order to unlock the vast potential of multivalent therapeutics.

References

1 M. Mammen, S.-K. Choi and G. M. Whitesides, *Angew. Chem., Int. Ed.*, 1998, **37**, 2754–2794.
2 W. J. Lees, A. Spaltenstein, J. E. Kingery-Wood and G. M. Whitesides, *J. Med. Chem.*, 1994, **37**, 3419–3433.
3 M. Mammen, G. Dahmann and G. M. Whitesides, *J. Med. Chem.*, 1995, **38**, 4179–4190.
4 Y. M. Chabre and R. Roy, *Adv. Carbohydr. Chem. Biochem.*, 2010, **63**, 165–393.
5 C. M. Paleos, D. Tsiourvas, Z. Sideratou and L.-A. Tziveleka, *Expert Opin. Drug Delivery*, 2010, **7**, 1387–1398.
6 P. H. Seeberger and D. B. Werz, *Nat. Rev. Drug Discovery*, 2005, **4**, 751–763.
7 L. L. Kiessling, J. E. Gestwicki and L. E. Strong, *Angew. Chem., Int. Ed.*, 2006, **45**, 2348–2368.
8 R. J. Pieters, *Org. Biomol. Chem.*, 2009, **7**, 2013–2025.
9 W. P. Jencks, *Proc. Natl. Acad. Sci. U. S. A.*, 1981, **78**, 4046–4050.
10 J. J. Lundquist and E. J. Toone, *Chem. Rev.*, 2002, **102**, 555–578.
11 P. I. Kitov and D. R. Bundle, *J. Am. Chem. Soc.*, 2003, **125**, 16271–16284.
12 E. T. Mack, P. W. Snyder, R. Perez-Castillejos, B. Bilgiçer, D. T. Moustakas, M. J. Butte and G. M. Whitesides, *J. Am. Chem. Soc.*, 2012, **134**, 333–345.
13 R. S. Kane, *Langmuir*, 2010, **26**, 8636–8640.
14 L. L. Kiessling, J. E. Gestwicki and L. E. Strong, *Curr. Opin. Chem. Biol.*, 2000, **4**, 696–703.
15 R. Subbiah, M. Veerapandian and K. S. Yun, *Curr. Med. Chem.*, 2010, **17**, 4559–4577.
16 J. M. Holub and K. Kirshenbaum, *Chem. Soc. Rev.*, 2010, **39**, 1325–1337.
17 A. D. Schlüter and J. P. Rabe, *Angew. Chem., Int. Ed.*, 2000, **39**, 864–883.

18 P. I. Kitov, J. M. Sadowska, G. Mulvey, G. D. Armstrong, H. Ling, N. S. Pannu, R. J. Read and D. R. Bundle, *Nature*, 2000, **403**, 669–672.
19 R. D. Astronomo, E. Kaltgrad, A. K. Udit, S.-K. Wang, K. J. Doores, C.-Y. Huang, R. Pantophlet, J. C. Paulson, C.-H. Wong, M. G. Finn and D. R. Burton, *Chem. Biol.*, 2010, **17**, 357–370.
20 B. D. Polizzotti and K. L. Kiick, *Biomacromolecules*, 2006, **7**, 483–490.
21 I. Papp, C. Sieben, K. Ludwig, M. Roskamp, C. Böttcher, S. Schlecht, A. Herrmann and R. Haag, *Small*, 2010, **6**, 2900–2906.
22 L. Gu, T. Elkin, X. Jiang, H. Li, Y. Lin, L. Qu, T.-R. J. Tzeng, R. Joseph and Y.-P. Sun, *Chem. Commun.*, 2005, 874–876.
23 V. Pavet, J. Beyrath, C. Pardin, A. Morizot, M.-C. Lechner, J.-P. Briand, M. Wendland, W. Maison, S. Fournel, O. Micheau, G. Guichard and H. Gronemeyer, *Cancer Res.*, 2010, **70**, 1101–1110.
24 B. Li, S. J. Russell, D. M. Compaan, K. Totpal, S. A. Marsters, A. Ashkenazi, A. G. Cochran, S. G. Hymowitz and S. S. Sidhu, *J. Mol. Biol.*, 2006, **361**, 522–536.
25 C. Fasting, C. A. Schalley, M. Weber, O. Seitz, S. Hecht, B. Koksch, J. Dernedde, C. Graf, E.-W. Knapp and R. Haag, *Angew. Chem., Int. Ed.*, 2012, **51**, 10472–10498.
26 S.-J. Richads, M. W. Jones, M. Hunaban, D. M. Haddleton and M. I. Gibson, *Angew. Chem., Int. Ed.*, 2012, **51**, 7812–7816.
27 C. Scheibe, A. Bujotzek, J. Dernedde, M. Weber and O. Seitz, *Chem. Sci.*, 2011, **2**, 770–775.
28 M. Taylor, S. Moore, J. Mayes, E. Parkin, M. Beeg, M. Canovi, M. Gobbi, D. M. A. Mann and D. Allsop, *Biochemistry*, 2010, **49**, 3261–3272.
29 J. C. Lee, K. A. Parker and N. S. Sampson, *J. Am. Chem. Soc.*, 2006, **128**, 4578–4579.
30 C. C. Lee, J. A. MacKay, J. M. J. Fréchet and F. C. Szoka, *Nat. Biotechnol.*, 2005, **23**, 1517–1526.
31 P. Schwab, R. H. Grubbs and J. W. Ziller, *J. Am. Chem. Soc.*, 1996, **118**, 100–110.
32 M. Scholl, S. Ding, C. W. Lee and R. H. Grubbs, *Org. Lett.*, 1999, **1**, 953–956.
33 J. A. Love, J. P. Morgan, T. M. Trnka and R. H. Grubbs, *Angew. Chem., Int. Ed.*, 2002, **41**, 4035–4037.
34 L. E. Strong and L. L. Kiessling, *J. Am. Chem. Soc.*, 1999, **121**, 6193–6196.
35 K. C. A. Garber, K. Wangkanont, E. E. Carlson and L. L. Kiessling, *Chem. Commun.*, 2010, **46**, 6747–6749.
36 R. H. Kramer and J. W. Karpen, *Nature*, 1998, **395**, 710–713.
37 M. Shan, A. Bujotzek, F. Abendroth, A. Wellner, R. Gust, O. Seitz, M. Weber and R. Haag, *ChemBioChem*, 2011, **12**, 2587–2598.
38 G. R. Newkome, C. N. Moorefield and F. Vögtle, *Dendrimers and Dendrons: Concepts, Synthesis, Applications*, Wiley-VCH, Weinheim, 2001.
39 D. Astruc, E. Boisseller and C. Ornelas, *Chem. Rev.*, 2010, **110**, 1857–1959.
40 O. M. Milhem, C. Myles, N. B. McKeown, D. Attwood and A. D'Emanuele, *Int. J. Pharm.*, 2000, **197**, 239–241.
41 R. K. Tekade, P. V. Kumar and N. K. Jain, *Chem. Rev.*, 2009, **109**, 49–87.
42 D. G. Mullen, M. Fang, A. Desai, J. Baker, Jr, B. G. Orr and M. M. Banaszak Holl, *ACS Nano*, 2010, **4**, 657–670.
43 Y.-H. Jiang, P. Emau, J. S. Cairns, L. Flanary, W. R. Morton, T. D. McCarthy and C.-C. Tsai, *AIDS Res. Hum. Retroviruses*, 2005, **21**, 207–213.
44 E. Gong, B. Matthews, T. D. McCarthy, J. Chu, G. Holan, J. Raff and S. Sacks, *Antiviral Res.*, 2005, **68**, 139–146.
45 J. O'Loughlin, I. Millwood, H. M. McDonald, C. F. Price, J. M. Kaldor and J. R. A. Paull, *Sex. Transm. Dis.*, 2010, **37**, 100–104.
46 S. Telwatte, K. Moore, A. Johnson, D. Tyssen, J. Sterjovski, M. Aldunate, P. R. Gorry, P. A. Ramsland, G. Lewis, J. R. A. Paull, S. Sonza and G. Tachedjian, *Antiviral Res.*, 2011, **90**, 195–199.
47 A. Luganini, S. F. Nicoletto, L. Pizzuto, G. Pirri, A. Giuliani, S. Landolfo and G. Gribaudo, *Antimicrob. Agents Chemother.*, 2011, **55**, 3231–3239.
48 M. A. Mintzer, E. L. Dane, G. A. O'Toole and M. W. Grinstaff, *Mol. Pharmaceutics*, 2012, **9**, 342–354.
49 J. P. Thompson and C.-L. Schengrund, *Glycoconjugate J.*, 1997, **14**, 837–845.
50 P. H. Fishman, T. Pacuszka and P. A. Orlandi, *Adv. Lipid Res.*, 1993, **25**, 165–187.
51 S. M. Janib, A. S. Moses and J. A. MacKay, *Adv. Drug Delivery Rev.*, 2010, **62**, 1052–1063.
52 S. Rana, A. Bajaj, R. Mout and V. M. Rotello, *Adv. Drug Delivery Rev.*, 2012, **64**, 200–216.
53 M. Elsabahy and K. L. Wooley, *Chem. Soc. Rev.*, 2012, **41**, 2545–2561.
54 Y.-J. Li, A. L. Perkins, Y. Su, Y. Ma, L. Colson, D. A. Horne and Y. Chen, *Proc. Natl. Acad. Sci. U. S. A.*, 2012, **109**, 4092–4097.
55 M. H. Tatham, M.-C. Geoffroy, L. Shen, A. Plechanovova, N. Hattersley, E. G. Jaffray, J. J. Palvimo and R. T. Hay, *Nat. Cell Biol.*, 2008, **10**, 538–546.
56 B. Peng, M. Locascio, P. Zapol, S. Li, S. L. Mielke, G. C. Schatz and H. D. Espinosa, *Nat. Nanotechnol.*, 2008, **3**, 626–631.
57 H. Dai, *Acc. Chem. Res.*, 2002, **35**, 1035–1044.
58 A. Montellano, T. Da Ros, A. Bianco and M. Prato, *Nanoscale*, 2011, **3**, 4035–4041.
59 H. S. Vieira, D. M. Andrada, R. Mendonça, A. P. Santos, M. D. Martins, W. A. A. Macedo, H. F. Gorgulho, L. P. S. Pimenta, R. L. Moreira, A. Jorio, M. A. Pimenta and C. A. Furtado, *J. Nanosci. Nanotechnol.*, 2007, **7**, 3412–3430.
60 C. Richard, F. Balavoine, P. Schultz, T. W. Ebbesen and C. Mioskowski, *Science*, 2003, **300**, 775–778.
61 H. Naeimi, A. Mohajeri, L. Moradi and A. Rashidi, *J. Nanosci. Nanotechnol.*, 2011, **11**, 8903–8906.
62 T. Premkumar, R. Mezzenga and K. E. Geckeler, *Small*, 2012, **8**, 1299–1313.
63 F. Balavoine, P. Schultz, C. Richard, V. Mallouh, T. W. Ebbesen and C. Mioskowski, *Angew. Chem., Int. Ed.*, 1999, **38**, 1912–1915.

64 R. J. Chen, Y. Zhang, D. Wang and H. Dai, *J. Am. Chem. Soc.*, 2001, **123**, 3838–3839.
65 M. Assali, M. P. Leal, I. Fernández, R. Baati, C. Mioskowski and N. Khiar, *Soft Matter*, 2009, **5**, 948–950.
66 C. R. Bertozzi and L. L. Kiessling, *Science*, 2001, **291**, 2357–2364.
67 N. Stephanopoulos, G. J. Tong, S. C. Hsiao and M. B. Francis, *ACS Nano*, 2010, **4**, 6014–6020.
68 J. K. Pokorski, M. L. Hovlid and M. G. Finn, *ChemBioChem*, 2011, **12**, 2441–2447.
69 J. Lucon, S. Qazi, M. Uchida, G. J. Bedwell, B. LaFrance, P. E. Prevelige, Jr and T. Douglas, *Nat. Chem.*, 2012, **4**, 781–788.
70 E. A. Anderson, S. Isaacman, D. S. Peabody, E. Y. Wang, J. W. Canary and K. Kirshenbaum, *Nano Lett.*, 2006, **6**, 1160–1164.
71 A. Datta, J. M. Hooker, M. Botta, M. B. Francis, S. Aime and K. N. Raymond, *J. Am. Chem. Soc.*, 2008, **130**, 2546–2552.
72 J.-M. Lehn, *Supramolecular Chemistry: Concepts and Perspectives*, Wiley-VCH, Weinheim, 1995.
73 A. Barnard and D. K. Smith, *Angew. Chem., Int. Ed.*, 2012, **51**, 6572–6581.
74 D. Grünstein, M. Maglinao, R. Kikkeri, M. Collot, K. Barylyuk, B. Lepenies, F. Kamena, R. Zenobi and P. H. Seeberger, *J. Am. Chem. Soc.*, 2011, **133**, 13957–13966.
75 M. K. Müller and L. Brunsveld, *Angew. Chem., Int. Ed.*, 2009, **48**, 2921–2924.
76 J. Geng, F. Biedermann, J. M. Zayed, F. Tian and O. A. Scherman, *Macromolecules*, 2011, **44**, 4276–4281.
77 J.-S. Zhang, F. Liu and L. Huang, *Adv. Drug Delivery Rev.*, 2005, **57**, 689–698.
78 R. Tarallo, A. Accardo, A. Falanga, D. Guarnieri, G. Vitiello, P. Netti, G. D'Errico, G. Morelli and S. Galdiero, *Chem.–Eur. J.*, 2011, **17**, 12659–12668.
79 K. Maruyama, *Adv. Drug Delivery Rev.*, 2011, **63**, 161–169.
80 M. Liu, K. Kono and J. M. J. Fréchet, *J. Controlled Release*, 2000, **65**, 121–131.
81 A. M. Nyström and K. L. Wooley, *Acc. Chem. Res.*, 2011, **44**, 969–978.
82 D. Wang, W. Liao and P. S. Arora, *Angew. Chem., Int. Ed.*, 2005, **44**, 6525–6529.
83 M. Mutter, P. Dumy, P. Garouste, C. Lehmann, M. Mathieu, C. Peggion, S. Peluso, A. Razaname and G. Tuchscherer, *Angew. Chem., Int. Ed. Engl.*, 1996, **35**, 1482–1485.
84 D. Boturyn, J.-L. Coll, E. Garanger, M.-C. Favrot and P. Dumy, *J. Am. Chem. Soc.*, 2004, **126**, 5730–5739.
85 J. R. Cochran and L. J. Stern, *Chem. Biol.*, 2000, **7**, 683–696.
86 S. P. Schoenberger, R. E. M. Toes, E. I. H. van der Voort, R. Offringa and C. J. M. Melief, *Nature*, 1998, **393**, 480–483.
87 S. R. M. Bennett, F. R. Carbone, F. Karamalis, R. A. Flavell, J. F. A. P. Miller and W. R. Heath, *Nature*, 1998, **393**, 478–480.
88 J.-L. Bodmer, P. Schneider and J. Tschopp, *Trends Biochem. Sci.*, 2002, **27**, 19–26.
89 A. D. Kirk, L. C. Burkly, D. S. Batty, R. E. Baumgartner, J. D. Berning, K. Buchanan, J. H. Fechner Jr, R. L. Germond, R. L. Kampen, N. B. Patterson, S. J. Swanson, D. K. Tadaki, C. N. TenHoor, L. White, S. J. Knechtle and D. M. Harlan, *Nat. Med.*, 1999, **5**, 686–693.
90 L. Diehl, A. T. den Boer, S. P. Schoenberger, E. I. H. van der Voort, T. N. M. Schumacher, C. J. M. Melief, R. Offringa and R. E. M. Toes, *Nat. Med.*, 1999, **5**, 774–779.
91 E. M. Sotomayor, I. Borrello, E. Tubb, F.-M. Rattis, H. Bien, Z. Lu, S. Fein, S. Schoenberger and H. I. Levitsky, *Nat. Med.*, 1999, **5**, 780–787.
92 S. Fournel, S. Wieckowski, W. Sun, N. Trouche, H. Dumortier, A. Bianco, O. Chaloin, M. Habib, J.-C. Peter, P. Schneider, B. Vray, R. E. M. Toes, R. Offringa, C. J. M. Melief, J. Hoebeke and G. Guichard, *Nat. Chem. Biol.*, 2005, **1**, 377–382.
93 D. I. Bryson, W. Zhang, P. M. McLendon, T. M. Reineke and W. L. Santos, *ACS Chem. Biol.*, 2012, **7**, 210–217.
94 M. Stevens, E. De Clercq and J. Balzarini, *Med. Res. Rev.*, 2006, **26**, 595–625.
95 J. R. Thomas and P. J. Hergenrother, *Chem. Rev.*, 2008, **108**, 1171–1224.
96 S. Hwang, N. Tamilarasu, K. Ryan, I. Huq, S. Richter, W. C. Still and T. M. Rana, *Proc. Natl. Acad. Sci. U. S. A.*, 1999, **96**, 12997–13002.
97 H.-Y. Mei, D. P. Mack, A. A. Galan, N. S. Halim, A. Heldsinger, J. A. Loo, D. W. Moreland, K. A. Sannes-Lowery, L. Sharmeen, H. A. Truong and A. W. Czarnik, *Bioorg. Med. Chem.*, 1997, **5**, 1173–1184.
98 J. S. Appelbaum, J. R. LaRochelle, B. A. Smith, D. M. Balkin, J. M. Holub and A. Schepartz, *Chem. Biol.*, 2012, **19**, 819–830.
99 K. Gorska, K.-T. Huang, O. Chaloin and N. Winssinger, *Angew. Chem., Int. Ed.*, 2009, **48**, 7695–7700.
100 M. Egholm, O. Buchardt, L. Christensen, C. Behrens, S. M. Freier, D. A. Driver, R. H. Berg, S. K. Kim, B. Norden and P. E. Nielsen, *Nature*, 1993, **365**, 566–568.
101 C. Gambacorti-Passerini, L. Mologni, C. Bertazzoli, P. le Coutre, E. Marchesi, F. Grignani and P. E. Nielsen, *Blood*, 1996, **88**, 1411–1417.
102 A. Dragulescu-Andrasi, S. Rapireddy, G. He, B. Bhattacharya, J. J. Hyldig-Nielsen, G. Zon and D. H. Ly, *J. Am. Chem. Soc.*, 2006, **128**, 16104–16112.
103 E. A. Englund, D. Wang, H. Fujigaki, H. Sakai, C. M. Micklitsch, R. Ghirlando, G. Martin-Manso, M. L. Pendrak, D. D. Roberts, S. R. Durell and D. H. Appella, *Nat. Commun.*, 2012, **3**, 614.
104 L. Auzzas, F. Zanardi, L. Battistini, P. Burreddu, P. Carta, G. Rassu, C. Curti and G. Casiraghi, *Curr. Med. Chem.*, 2010, **17**, 1255–1299.
105 J. A. Nemeth, M. T. Nakada, M. Trikha, Z. Lang, M. S. Gordon, G. C. Jayson, R. Corringham, U. Prabhakar, H. M. Davis and R. A. Beckman, *Cancer Invest.*, 2007, **25**, 632–646.
106 L. W. Dobrucki and A. J. Sinusas, *Curr. Opin. Biotechnol.*, 2007, **18**, 90–96.
107 C. B. Carlson, P. Mowery, R. M. Owen, E. C. Dykhuizen and L. L. Kiessling, *ACS Chem. Biol.*, 2007, **2**, 119–127.
108 J. L. Childs-Disney, P. B. Tsitovich and M. D. Disney, *ChemBioChem*, 2011, **12**, 2143–2146.

109 R. N. Zuckermann, J. M. Kerr, S. B. H. Kent and W. H. Moos, *J. Am. Chem. Soc.*, 1992, **114**, 10646–10647.
110 J. R. Stringer, J. A. Crapster, I. A. Guzei and H. E. Blackwell, *J. Org. Chem.*, 2010, **75**, 6068–6078.
111 N. H. Shah, G. L. Butterfoss, K. Nguyen, B. Yoo, R. Bonneau, D. L. Rabenstein and K. Kirshenbaum, *J. Am. Chem. Soc.*, 2008, **130**, 16622–16632.
112 J. R. Stringer, J. A. Crapster, I. A. Guzei and H. E. Blackwell, *J. Am. Chem. Soc.*, 2011, **133**, 15559–15567.
113 A. S. Culf and R. J. Ouellette, *Molecules*, 2010, **15**, 5282–5335.
114 B. Yoo and K. Kirshenbaum, *Curr. Opin. Chem. Biol.*, 2008, **12**, 714–721.
115 K. T. Nam, S. A. Shelby, P. H. Choi, A. B. Marciel, R. Chen, L. Tan, T. K. Chu, R. A. Mesch, B.-C. Lee, M. D. Connoly, S. Kisielowski and R. N. Zuckermann, *Nat. Mater.*, 2010, **9**, 454–460.
116 N. C. Tan, P. Yu, Y.-U. Kwon and T. Kodadek, *Bioorg. Med. Chem.*, 2008, **16**, 5853–5861.
117 S. M. Miller, R. J. Simon, S. Ng, R. N. Zuckermann, J. M. Kerr and W. H. Moos, *Drug Dev. Res.*, 1995, **35**, 20–32.
118 Y. Lee and N. S. Sampson, *Curr. Opin. Struct. Biol.*, 2006, **16**, 544–550.
119 H. Jang, A. Fafarman, J. M. Holub and K. Kirshenbaum, *Org. Lett.*, 2005, **7**, 1951–1954.
120 J. M. Holub, H. Jang and K. Kirshenbaum, *Org. Biomol. Chem.*, 2006, **4**, 1497–1502.
121 S. A. Fowler and H. E. Blackwell, *Org. Biomol. Chem.*, 2009, **7**, 1508–1524.
122 R. M. Evans, *Science*, 1988, **240**, 889–895.
123 F. Schaufele, X. Carbonell, M. Guerbadot, S. Borngraeber, M. S. Chapman, A. A. K. Ma, J. N. Miner and M. I. Diamond, *Proc. Natl. Acad. Sci. U. S. A.*, 2005, **102**, 9802–9807.
124 M. M. Centenera, J. M. Harris, W. D. Tilley and L. M. Butler, *Mol. Endocrinol.*, 2008, **22**, 2373–2382.
125 D. Gioeli, S. B. Ficarro, J. J. Kwiek, D. Aaronson, M. Hancock, A. D. Catling, F. M. White, R. E. Christian, R. E. Settlage, J. Shabanowitz, D. F. Hunt and M. J. Weber, *J. Biol. Chem.*, 2002, **277**, 29304–29314.
126 J. M. Holub, M. J. Garabedian and K. Kirshenbaum, *QSAR Comb. Sci.*, 2007, **26**, 1175–1180.
127 J. M. Holub, M. J. Garabedian and K. Kirshenbaum, *Mol. BioSyst.*, 2011, **7**, 337–345.
128 P. M. Levine, K. Imberg, M. J. Garabedian and K. Kirshenbaum, *J. Am. Chem. Soc.*, 2012, **134**, 6912–6915.
129 C. Tran, S. Ouk, N. J. Clegg, Y. Chen, P. A. Watson, V. Arora, J. Wongvipat, P. M. Smith-Jones, D. Yoo, A. Kwon, T. Wasielewska, D. Welsbie, C. D. Chen, C. Higano, T. M. Beer, D. T. Hung, H. I. Scher, M. E. Jung and C. Sawyers, *Science*, 2009, **324**, 787–790.
130 P. M. Levine, E. Lee, A. Greenfield, R. Bonneau, S. K. Logan, M. J. Garabedian and K. Kirshenbaum, *ACS Chem. Biol.*, 2012, **7**, 1693–1701.
131 L. Guan and M. D. Disney, *ACS Chem. Biol.*, 2012, **7**, 73–86.
132 A. Mankodi, E. Logigian, L. Callahan, C. McClain, R. White, D. Henderson, M. Krym and C. A. Thornton, *Science*, 2000, **289**, 1769–1772.
133 C. L. Liquori, K. Ricker, M. L. Moseley, J. F. Jacobsen, W. Kress, S. L. Naylor, J. W. Day and L. P. W. Ranum, *Science*, 2001, **293**, 864–867.
134 L. P. W. Ranum and T. A. Cooper, *Annu. Rev. Neurosci.*, 2006, **29**, 259–277.
135 J. D. Brook, M. E. McCurrach, H. G. Harley, A. J. Buckler, D. Church, H. Aburtani, K. Hunter, V. P. Stanton, J.-P. Thirion, T. Hudson, R. Sohn, B. Zemelman, R. G. Snell, S. A. Rundle, S. Crow, J. Davies, P. Shelbourne, J. Buxton, C. Jones, V. Juvonen, K. Johnson, P. S. Harper, D. J. Shaw and D. E. Housman, *Cell*, 1992, **68**, 799–808.
136 J. Cho and R. R. Rando, *Nucleic Acids Res.*, 2000, **28**, 2158–2163.
137 A. Pushechnikov, M. M. Lee, J. L. Childs-Disney, K. Sobczak, J. M. French, C. A. Thornton and M. D. Disney, *J. Am. Chem. Soc.*, 2009, **131**, 9767–9779.
138 J. L. Childs-Disney, J. Hoskins, S. G. Rzuczek, C. A. Thornton and M. D. Disney, *ACS Chem. Biol.*, 2012, **7**, 856–862.
139 M. M. Lee, A. Pushechnikov and M. D. Disney, *ACS Chem. Biol.*, 2009, **4**, 345–355.
140 M. M. Lee, J. L. Childs-Disney, A. Pushechnikov, J. M. French, K. Sobczak, C. A. Thornton and M. D. Disney, *J. Am. Chem. Soc.*, 2009, **131**, 17464–17472.